Capillarity

Vol. 8, No. 3, p. 45-52, 2023

Original article

Impact of capillary pressure on micro-fracture propagation pressure during hydraulic fracturing in shales: An analytical model

Yunhu Lu[1,2]*, Yan Jin[1,2], Hongda Li[2]

[1]*National Key Laboratory of Petroleum Resources and Engineering, China University of Petroleum (Beijing), Beijing 102249, P. R. China*
[2]*College of Petroleum Engineering, China University of Petroleum (Beijing), Beijing 102249, P. R. China*

Keywords:
Shale reservoirs
micro-fractures
propagation pressure
capillary pressure
wettability

Cited as:
Lu, Y., Jin, Y., Li, H. Impact of capillary pressure on micro-fracture propagation pressure during hydraulic fracturing in shales: An analytical model. Capillarity, 2023, 8(3): 45-52.
https://doi.org/10.46690/capi.2023.09.01

Abstract:
The presence of micro-fractures in shale reservoirs is vital for economic production. While a number of models have been proposed to predict the propagation pressure of pre-existing micro-fractures, few models have considered capillary pressure, which may play a significant role in the presence of micro-fractures with nano-scale width. In this study, a new model was developed to predict the propagation pressure of micro-fractures. It is assumed that pre-existing micro-fractures are arbitrarily intersected with the propagated hydraulic fractures. The model was derived based upon linear elastic fracture mechanics under the condition of mode I fracture propagation coupled with capillary pressure. Furthermore, this paper also conducted sensitivity analyses to predict the micro-fracture propagation pressure as a function of the contact angle, surface tension and the width of micro-fracture. The results demonstrated that decreasing the contact angle reduces the propagation pressure of micro-fractures, implying that a hydrophilic system may yield a lower fracture propagation pressure compared with the hydrophobic counterpart. Moreover, for a hydrophilic system, further decreasing the contact angle shifts the propagation pressure to a negative value, implying that the capillary pressure may induce the propagation of micro-fractures without external fluid injection. The propagation pressure is also affected by the surface tension and the width of micro-fracture.

1. Introduction

Unconventional shale oil and gas have revolutionized the energy landscape in the United States and the world due to the decline in conventional resources (Wang et al., 2014; Roshan et al., 2016). Owing to the extremely low permeability of shale, a combination of horizontal drilling and multi-stage hydraulic fracturing technology are generally utilized for economic production. Apart from hydraulic fractures, shale plays are quite often naturally fractured reservoirs with a size ranging from the micrometre (i.e., micro-fracture) to the kilometre scale (Gale et al., 2007, 2014; Curtis et al., 2010; Liu et al., 2022), which provides pathways to transport oil and/or gas from the matrix to hydraulic fractures (Wang et al., 2016; Feng et al., 2020; Liu et al., 2022). However, these natural fractures may not be internally connected with each other near the wellbore or hydraulic fractures, which in turn constrains the conductivity of natural fractures. Therefore, it is essential to explore the potential of the reactivation and propagation of micro-fractures during the hydraulic fracture stimulation.

Since the inception of hydraulic fracturing in conventional reservoirs, the mechanisms of the propagation of hydraulic fractures are well-established phenomena. According to the classical mechanism, the extension of hydraulic fractures and the characteristics of the interaction among initiated hydraulic fracture, pre-exiting natural fractures and induced natural

*Corresponding author.
E-mail address: luyh@cup.edu.cn (Y. Lu); jiny@cup.edu.cn (Y. Jin); lhd1792092303@163.com (H. Li).

Yandy Scientific Press

2709-2119
Received June 29, 2023; revised July 18, 2023; accepted August 5, 2023; available online August 9, 2023.

fractures of all sizes depend on various factors, which include the rock mechanical properties, fracturing fluid properties, reservoir fluid, and natural fracture properties (e.g., geometry, size orientation) (Fatahi et al., 2016; Fallahzadeh et al., 2017; Fatahi and Sarmadivaleh, 2017; Feng et al., 2018), state of stresses (e.g., in-situ stresses, differential stresses, stress regime etc.) (Hossain et al., 2000; Rahman et al., 2002; Hossain and Rahman, 2008), and rock and fluid interactions mechanisms (Kumagai and Chouet, 2000; Rahman et al., 2000; Hou et al., 2018; Peng et al., 2018; Feng and Chen, 2019).

Despite the above achievements, the effect of capillary pressure (especially at the tip of hydraulic fractures) on the hydraulic fracture propagation pressure has not been examined, since the capillary pressure effect at the very small scale of hydraulic fracture tip is generally assumed to be negligible. However, some authors hypothesized that capillary pressure (with nano-scale of natural fracture tip) plays a significant role in increasing the stress intensity factor, thus decreasing the micro-fracture propagation pressure (Wang et al., 2016; Lu et al., 2018). Previous studies have shown that multiphase flows in porous media are in a transient state with the dynamic effect in capillary pressure and focus on the measurement of dynamic effect in capillary pressure (Li et al., 2022). Meanwhile, capillary imbibition and fluid flow in porous systems driven by capillary pressure are also the most ubiquitous phenomena in nature and industry, including petroleum and hydraulic engineering (Cai et al., 2014, 2021, 2022). Therefore, there is a pressing need to incorporate the capillary pressure effect into predicting the propagation pressure of micro-fractures in shale. If this physical process takes place during hydraulic fracture propagation in shales, pre-existing natural micro-fractures, which intersect with the propagated hydraulic fractures, could potentially be activated through the propagation of micro-fractures due to the influence of capillary pressure. Consequently, in addition to the creation of new fractures, the re-activation of pre-existing natural fractures of all sizes during the propagation of hydraulic fractures may also play a significant role in enhancing the interconnectivity and thus the productivity. This is because the interconnected fractures provide pathways that improve the hydraulic fracture conductivity through allowing the better transportation of reservoir fluids from matrix to hydraulic fractures to the wellbore, enhancing the well production performance (Mayerhofer et al., 2010; Gandossi and Von Estorff, 2013). In addition, the capillary pressure has been experimentally shown to cause a major change in the strength of various rocks (such as shale, chalk, limestone, sandstone, gypsum, mudrock, etc.) (Priest and Selvakumar, 1982; Yilmaz, 2010). To explain the capillary effects, Bishop (1959) experimentally introduced a generalized effective stress established on soils partially saturated with air and water. Bishop's effective stress was also applied to explain the strength and deformation of partially saturated rocks (Fjær et al., 2008; Silva et al., 2008) and solids. Verdugo and Doster (2022) analysed the impact of capillary pressure on hydraulically fractured tight gas wells with the objective of understanding the clean-up process at reservoir level and its impact on future well performance.

In order to verify the hypothesis outlined above, authors previously developed an analytical model with the assumption that micro-fractures in tight sandstone reservoirs are orthogonal to hydraulic fractures (Lu et al., 2019). The current study is the extension of that work. It puts an emphasis on the pre-exiting natural micro-fractures, which are intersected arbitrarily with the propagated hydraulic fractures. However, to better represent the distribution of natural micro-fractures in shale reservoirs, the previous analytical model was updated to consider micro-fractures arbitrarily intersected with hydraulic fractures. In addition, given that shale reservoirs exhibit a strong heterogeneity in wettability, it is necessary to examine the effect of capillary pressure on micro-fracture propagation in hydrophilic (inorganic materials) and hydrophobic (organic systems, i.e., organic matter) systems together with the interfacial tension and the width of micro-fracture tip.

2. Methodology

2.1 Model for the propagation of pre-existing natural micro-fractures

In order to interpret the effect of capillary pressure on the propagation of a pre-existing natural micro-fracture arbitrarily intersected with hydraulic fracture, this study was performed based on the mechanics of linear hydro-fracture, which delineates the driving factor(s) in this process. To further predict the propagation of natural micro-fractures intersected with the generated hydraulic fracture, a mathematical model in light of the mechanics of linear elastic fracture (Rahman et al., 2000) was developed on the basis of a conceptual mode, as shown in Fig. 1.

As presented in the above figure, in-situ natural micro-fractures arbitrarily intersect a hydraulic fracture with an angle β. This is the orientation of micro-fracture, that is, the angle between micro-fracture and the direction of minimum principal horizontal in-situ stress. The parameters a_u and a_d represent the upper and lower sides of the incremental extension length of hydraulic fracture. It is assumed that the micro-fracture intersecting with the main hydraulic fracture can propagate under the capillary pressure. l_{nu}, and l_{nd} are respectively the upper and lower side of the micro-fracture without any contribution from the hydraulic fracture. L_{nu}, and L_{nd} are respectively the total half-lengths of the micro-fracture.

Fig. 1 further shows the distribution of fluids and pressures in the hydraulic fractures and micro-fractures in a two-dimensional view. The blue horizontal column represents the fracturing fluid in the hydraulic fracture, and the orange inclined cylinder represents the pre-existing formation fluid, typically shale oil or gas. The half-length of hydraulic fracture is denoted by L. As aforementioned, the injected fluid can potentially enter the micro-fracture under external pressure, and the length of this part of fluids is represented by the blue inclined cylinder in Fig. 1.

The fracturing fluid then enters these fractures under the high injection pressure. Subsequently, the capillary pressure is induced at the water-hydrocarbon-rock interface when the injected fluid contacts with the pre-existing formation brine and hydrocarbon. As a result, the existing micro-fractures may extend and propagate under fluid-injection pressure and

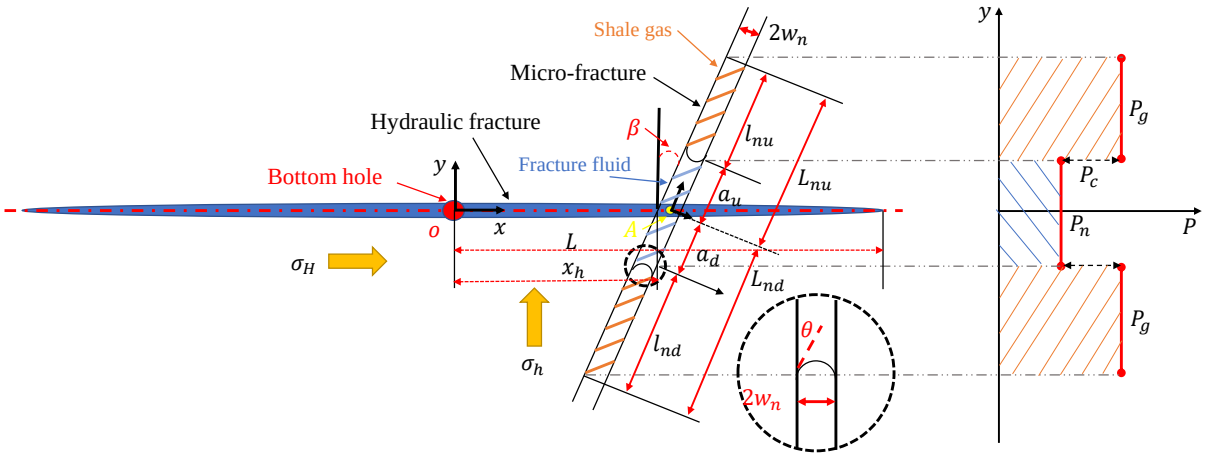

Fig. 1. Schematic of pressure distribution in pre-existing micro-fracture that is intersected with the main fracture after the hydraulic fracturing process.

capillary pressure depending on the stress intensity developed at the micro-fracture tip due to the resultant effect of hydraulic fracture fluid and capillary pressure, as well as the local stress system. If it is assumed that the pressure drop of fluid flow inside the micro-fractures is negligible, the system pressure can be divided into two parts: (i) the fluid injection pressure, which is equal to the pressure at the intersection between the main hydraulic fracture and induced micro-fracture; and (ii) the intrinsic pressure of the formation fluid, which is related to the resultant effect of in-situ stress. The difference between these two pressures is the capillary pressure.

In order to derive the proper analytical model, it is reasonable to make the same assumptions as in our previous study to calculate the intensity factor change, which is affected by capillary pressure mainly due to the wettability change. The details of modeling assumptions and limitations can be found in Lu et al. (2019).

2.2 Pressure in the fractures

In Fig. 1, the fluid pressure at any position in the hydraulic fracture can be obtained by using the classical Perkins-Kern-Nordgren fracture model (Hubbert and Willis, 1972):

$$P_h = P_w - \frac{256\mu QG^3}{\pi H^4(1-\nu)^3}x_h \tag{1}$$

where x_h represents the distance between the point where the micro-fracture intersects with the main fracture and the wellbore bottom hole in m (in Fig. 1, wellbore bottom hole refers to a point from which the hydraulic fracture is initiated); P_h represents the pressure at x_h inside the fracture in MPa; P_w represents the wellbore bottom hole pressure in MPa; Q represents the volumetric rate of fracturing fluid (or injection rate) in m^3/min; μ represents the viscosity of the fracturing fluid in mPa·s; G represents the shear modulus of shale reservoir in GPa; ν represents the Poisson's ratio; H is the formation thickness in m.

Inside the micro-fracture, the pressure of injected fluid is equal to the pressure of hydraulic fracture P_h at the point where it intersects with a micro-fracture, so the net pressure P_n of the fracturing fluid in the micro-fracture can be expressed by:

$$P_n = P_h - \frac{\sigma_H - \sigma_h}{2}(\cos 2\beta + 1) \tag{2}$$

where σ_H and σ_h denote the maximum and the minimum horizontal stress in MPa; β denote the orientation of micro-fracture.

The capillary pressure is induced when the injected fluids inside the micro-fracture contact with the pre-existing formation fluids. Under this condition, the net pressure P_g of the in-situ fluids is greater than the net pressure P_n of the injected fracturing fluid. The difference between these two net pressures is expressed by the capillary pressure (Lu et al., 2019). Thus:

$$P_g = P_n + P_c \tag{3}$$

The capillary pressure P_c is given by:

$$P_c = \frac{2\sigma\cos\theta}{w_n} \tag{4}$$

where P_c is given in MPa, σ represents the gas-liquid surface tension for the inside of micro-fracture in mN/m; θ is the contact angle between the fracturing fluid and the formation rock in °; w_n denotes the half width of micro-fracture in m.

2.3 Stress intensity factor at the tip of micro-fracture

Given that the main hydraulic fracture is intersected with the micro-fractures as shown in Fig. 1, it is not possible to directly use the traditional linear elastic method, which is based on the internal pressure distribution inside the fractures for the calculation of the stress intensity factor at the tip of the fracture. In this work, the stress intensity factor is derived from the linear elastic fracture mechanics and is used as the criterion to predict the propagation behaviour of micro-fractures. It is assumed that the hydraulic fracture only extends along the direction of maximum principal stress in the same

plane following the mode I (i.e., tensile fracture) fracture propagation criteria. Hence, the stress intensity factor at the hydraulic fracture tip K_{ih}, can be expressed by:

$$K_{ih} = \frac{0.806G\sqrt{\pi}}{2(1-v)\sqrt{\Delta a}} w_{tip} \tag{5}$$

where w_{tip} represents the opening displacement of the micro-fracture tip, which is generally termed as the width of micro-fracture in nm; Δa is the unit length of hydraulic fracture tip in m. From Eq. (1), the fluid pressure at the tip of the hydraulic fracture could de derived. The width of fracture tip under this pressure condition is then calculated by (Perkins and Kern, 1961):

$$w_{tip} = \frac{H(1-v)}{G}(P_h - \sigma_h) \tag{6}$$

According to the linear elastic fracture mechanics, the hydraulic fracture will extend and start propagating when the stress intensity factor at the hydraulic fracture tip, K_{ih}, is exceeded or is equal the fracture toughness of shale formation, K_{ic} (i.e., $K_{ih} \geq K_{ic}$). By applying this criterion, the hydraulic fracture propagation pressure p_{hp} can be obtained using Eqs. (1), (5) and (6), as given by:

$$p_{hp} = \frac{1.4\sqrt{\Delta a}K_{ic}}{H} + \sigma_h + \frac{256\mu QG^3}{\pi H^4(1-v)^3}x_h \tag{7}$$

For any micro-fracture that intersects with the hydraulic fracture, it is assumed that this micro-fracture is independent and not influenced by the other surrounding micro-fractures. Besides, only the rupture at the tip of micro-fracture is considered. Therefore, the stress intensity factor at the micro-fracture tip K_i, is given by (Rice, 1968; Adachi, 2001):

$$K_i = 2\sqrt{\frac{L}{\pi}}\int_0^L \frac{P(x)}{\sqrt{L^2-x^2}}\mathrm{d}x \tag{8}$$

where L represents the arbitrary half-length of micro-fracture in m; x represents the distance of a given point at the tip of micro-fracture to the point of the intersection between hydraulic fracture and micro-fracture in m; and $P(x)$ denotes the fluid pressure in the micro-fracture in MPa.

Substituting Eqs. (2)-(4) into Eq. (8) yields Eq. (9), which predicts the stress intensity factor at the micro-fracture tip:

$$K_i = 2\sqrt{\frac{L_{nu}}{\pi}}\left(\int_0^{a_u}\frac{P_n}{\sqrt{L_{nu}^2-x^2}}\mathrm{d}x + \int_{a_u}^{l_{nu}}\frac{P_g}{\sqrt{L_{nu}^2-x^2}}\mathrm{d}x\right) \tag{9}$$

When applying the fracture propagation criterion as described earlier, the propagation pressure of micro-fractures p_{np}, can be obtained by using Eqs. (1)-(4) and (9), as given by:

$$\begin{aligned} p_{np} = {} & \frac{K_{ic}}{\sqrt{\pi L_{nu}}} + \left(\frac{2}{\pi}\arcsin\frac{a_u}{L_{nu}} - 1\right)P_c \\ & + \frac{(R-1)\sigma_h}{2}(1+\cos 2\beta) + \frac{256\mu QG^3}{\pi H^4(1-v)^3}x_h \end{aligned} \tag{10}$$

where R is the non-uniform coefficient of in-situ stress, which is defined as $R = \sigma_H/\sigma_h$.

Consequently, the pressure variation obtained from Eqs. (7) and (10). Eq. (10) shows that the micro-fracture propagation pressure predominantly depends on the mechanical properties of the rock, the non-uniform coefficient of in-situ stress (R), the in-situ wettability of the fluid-rock system (θ), the orientation of micro-fracture (β), and the geometrical parameters of the hydraulic and micro-fractures.

Table 1. Input parameters used in the geomechanical model to estimate the stress intensity factor.

Parameter	Value
Formation thickness, m	50
Stratigraphic shear modulus, GPa	20
Poisson-Pine ratio	0.25
Fracture toughness, MPa·$\sqrt{\mathrm{m}}$	1.2
Maximum horizontal stress, MPa	42
Minimum horizontal stress, MPa	40
The orientation of micro-fracture, °	0-90
Fluid injection rate, m^3/min	2.5
Viscosity of injection fluid, mPa·s	2
Contact angle, °	0-180
Surface tension, mN/m	20-40
Half width of pre-existing micro-fracture, nm	10-50

2.4 Case study

In this part, the analytical model presented earlier is employed to investigate the effect of capillary pressure on the propagation of micro-fractures. Since capillary pressure is the function of contact angle (θ), surface tension (σ) and half width of the micro-fracture tip (w_n) (Eq. (4)), the propagation pressure as a function of these parameters (i.e., θ, σ and w_n) could be calculated. Table 1 provides the input parameters used in this work to estimate the stress intensity factor, with a focus on investigating the effect of contact angle (0°-180°), interfacial tension, and half width of the pre-existing fracture (10, 30 and 50 nm).

3. Results and discussion

3.1 Effect of contact angle and surface tension on the stress intensity factor

As mentioned earlier, the micro-fracture will propagate when the stress intensity factor K_i exceeds the fracture toughness. The stress intensity factor calculated by employing our developed model is presented Fig. 2 as a function of contact angle at different surface tensions for a micro-fracture of 10 nm width. To better interpret how the K_i can be influenced by capillary pressure, the hydrostatic pressure at the bottom hole (i.e., at the hydraulic fracture initiation point on wellbore) is set to zero in order to allow the spontaneous imbibition process. The width of micro-fracture is considered in this case to be 10 nm. As can be seen in Fig. 2, the stress intensity factor decreases with increasing contact angle for any surface tension. For instance, K_i is observed to drop from 13.17 to

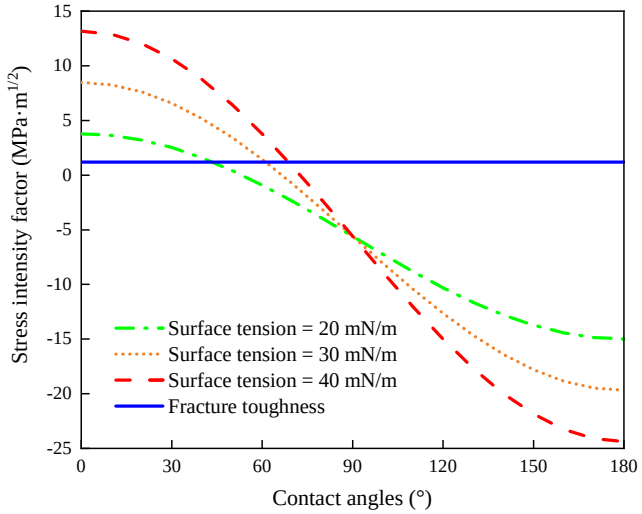

Fig. 2. Stress intensity factor as a function of contact angle at different surface tensions for micro-fracture with 10 nm width.

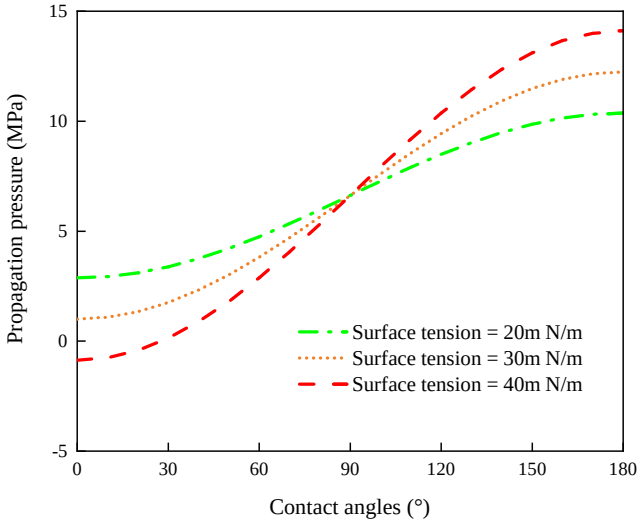

Fig. 3. The propagation pressure as a function of contact angle under different surface tensions for a 10 nm micro-fracture.

-24.38 MPa·$\sqrt{m}$ when the contact angle is increased from 0°-180° for a surface tension of 40 mN/m. Fig. 2 also shows that the value of K_i is greater than the fracture toughness (1.2 MPa·$\sqrt{m}$), while the contact angle is less than 70°, which implies that the propagation of micro-fracture will potentially occur under the water-wet condition.

Fig. 2 also shows that the value of K_i is higher with a larger surface tension when the contact angle is less than 90°, while on the contrary, it decreases when the contact angle is greater than 90°. For example, at a contact angle of 30°, K_i increases from 2.52-10.65 MPa·$\sqrt{m}$ when the surface tension increases from 20-40 mN/m. This means that for hydrophilic shale formation, increasing the surface tension will promote the propagation of existing micro-fractures. However, in the case of hydrophobic shale formation, high surface tension will further decrease the K_i, which can make it harder for an existing micro-fracture to propagate.

3.2 Effect of contact angle and surface tension on the propagation pressure

The propagation pressure as a function of contact angle at different surface tensions for a 10 nm micro-fracture is calculated using the developed model and shown in Fig. 3. It can be seen from the figure that the micro-fracture propagation pressure decreases with a decreasing contact angle for a given surface tension. For example, at an interfacial tension of 40 mN/m, the contact angle decreasing from 180°-0° leads to a reduction in propagation pressure from 14.11 to -0.87 MPa. It is worth noting that the negative propagation pressure means that the micro-fracture may propagate even without external fluid injection. Given that shale exhibits a strong heterogeneity in wettability with respect to the type and distribution of organic matter, these results indicate the possible contribution of capillary pressure to the propagation of pre-existing small micro-fractures (with nano-scale size) in water-wet shale, mainly in the areas that are rich in inorganic materials, whereas capillary pressure possibly increases the propagation pressure in oil-wet shale, mainly in the organic rich areas. The above results are consistent with those reported in the literature (Wang et al., 2015; Shen et al., 2016; Zhou et al., 2016).

Fig. 3 also indicates that the wettability shifting towards hydrophilicity may promote the propagation of a pre-existing micro-fracture due to the decrease in capillary pressure. Research has shown that low-salinity slick water for hydraulic fracturing could alter the in-situ wettability to more water-wet (Chen et al., 2018a, 2018b), favouring fluid uptake because of the capillary pressure, which acts as a diving force. Fig. 3 provides theoretical evidence that slick water may also trigger a decrease in the propagation pressure of pre-existing micro-fracture due to the wettability alteration towards more water-wet. This is well supported by the work of Xu and Dehghanpour (2014), who conducted spontaneous imbibition tests using intact shale samples in the presence of various brines. They reported that lowering the NaCl salinity would further dismantle shale samples and increase the water imbibition. Taken together, our results suggest that a shift in wettability towards more water-wet can decrease the propagation pressure, which can eventually lead to the re-activation as well as promote the propagation of micro-fractures.

The effect of surface tension on propagation pressure highly depends on the in-situ wettability (Fig. 3). In a hydrophilic system, increasing surface tension decreases the propagation pressure, whereas in a hydrophobic system, this trend is reversed. For example, for a contact angle of 40o, increasing the surface tension from 20-40 mN/m decreases the propagation pressure from 3.75-0.88 MPa. This indicates that increasing the fluid surface tension may induce the propagation of micro-fracture in a hydrophilic system. Our prediction is found to be in good agreement with the results of Dehghanpour et al. (2013) who simulated the hydraulic fracturing process using fluids with different surface tensions. They reported that increasing the fluid surface tension can decrease the formation propagation pressure, thus contributing to the enhancement of the volume of stimulated reservoirs in agreement with Fig. 2. However, Fig. 2 also indicates that, for a hydrophobic system,

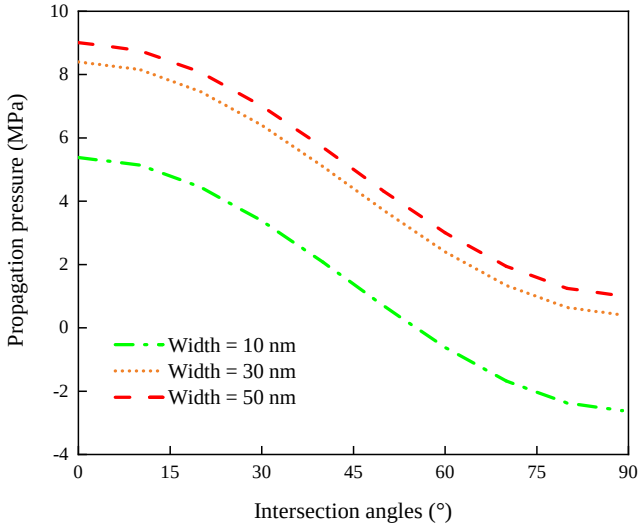

Fig. 4. Propagation pressure as a function of intersection angles for different widths of micro-fracture.

increasing the surface tension impedes the effectiveness of hydraulic fracturing because the capillary pressure acts as a resistance for micro-fracture propagation. These results collectively suggest that the wettability and interfacial tension may significantly influence the propagation pressure, which is associated with capillary pressure.

3.3 Effect of orientation and width of micro-fracture on the propagation pressure

The propagation pressure of micro-fractures, as a function of intersection angles for different widths of micro-fracture, plotted in Fig. 4, decreases with increasing the orientation angle between the micro-fracture and the direction minimum horizontal in-situ stress. In this study, the orientation 0° refers to a micro-fracture that is perpendicular to the direction of hydraulic fractures (i.e., the micro-fracture is parallel to the minimum horizontal stress), whereas 90° refers to micro-fracture parallel to the hydraulic fracture direction (micro-fracture is parallel to the maximum horizontal stress). As shown in Fig. 4, for the micro-fracture with 10 nm width, the increasing fracture orientation from 0°-80° decreases the propagation pressure from 5.38 to -2.61 MPa. Subsequently, the micro-fracture propagates along the direction of maximum horizontal stress. This is largely because the micro-fracture may not propagate until the propagation pressure exceeds the minimum horizontal stress, while the fractures parallel to the minimum horizontal stress need to overcome the maximum horizontal stress, leading to a higher propagation pressure. It is worth noting that the propagation pressure shifts to a negative value when the angle is greater than 55° under micro-fracture width of 10 nm or less, which implies that the capillary pressure can facilitate the re-activation as well as extension of micro-fracture, and thus potentially enhance oil/gas production through improving the formation connectivity (Wattenbarger and Alkouh, 2013).

For a constant orientation, the propagation pressure increases with the increasing width of micro-fracture. For example, for an angle of 70°, increasing the width from 10-50 nm shifts the propagation pressure from -1.98 to 1.94 MPa. This further supports that capillary pressure can potentially play a significant role in fracture propagation pressure. The increasing width of micro-fracture decreases the capillary pressure, thereby increasing the fracture propagation pressure (Liang et al., 2014).

4. Conclusions

In this work, a new analytical model was developed to discuss the impact of capillary pressure on the propagation pressure of micro-fractures. In particular, this paper considered that the pre-existing micro-fracture arbitrarily intersected with the hydraulic fracture better represents the distribution of micro-fractures in shale reservoirs. Moreover, given that shale reservoirs exhibit a strong heterogeneity in wettability, the effect of capillary pressure on micro-fracture propagation in hydrophilic (inorganic materials) and hydrophobic (organic matter) systems together with interfacial tension and the width of micro-fracture tip was also examined. Based on this analysis, the following conclusions are made:

1) For a hydrophilic system, the capillary pressure at the tip of micro-fractures could serve as a driving force that may significantly decrease the fracture propagation pressure. Theoretically, micro-fracture propagation pressure could be less than 0 MPa, which means that the capillary pressure could act as a main force to propagate micro-fractures with an assumption that the frictional force of fluids in micro-fractures is negligible. This suggests that under the condition of constant injection pressure, it can potentially induce the propagation of micro-fractures.
2) For a hydrophobic system (organic materials, i.e., organic matter), the propagation pressure of micro-fractures may rise with increasing hydrophobicity and fluid surface tension. This is because the capillary pressure could act as a dragging force and hinder the propagation of micro-fracture. This implies that special consideration needs to be given for the design of hydraulic fracturing fluids for organic-rich shale to enable the reactivation and propagation of interacting natural micro-fracture.
3) Micro-fracture width and intersection angle between micro-fractures and hydraulic fractures also play significant roles in the micro-fracture propagation pressure. The smaller the micro-fracture width, the higher the capillary pressure, which means that the wetting of the injected fluid can promote the extension of micro-fracture.
4) The greater the orientation angle between the micro-crack and the direction of minimum horizontal in-situ stress (i.e., micro-fractures that are more aligned with the main hydraulic fracture direction), the smaller the fracture pressure. This warrants that the intersected micro-fractures that are more aligned with the main hydraulic fractures are more likely to be activated and propagated upon the influence of capillary pressure. This can provide technical guidance for the optimization of hydraulic fracture stimulation tasks for shale reservoirs.

Acknowledgements

The authors acknowledge the financial support of the National Key Research and Development Program of China (No. 2019YFA0708303-05) and the National Natural Science Foundation of China (No. 52074314).

Conflict of interest

The authors declare no competing interest.

References

Adachi, J. I. Fluid-driven fracture in permeable rock. Minneapolis, University of Minnesota, 2001.

Bishop, A. W. The principle of effective strength. Teknisk Ukeblad, 1959, 106(39): 859-863.

Cai, J., Chen, Y., Liu, Y., et al. Capillary imbibition and flow of wetting liquid in irregular capillaries: A 100-year review. Advances in Colloid and Interface Science, 2022, 304: 102654.

Cai, J., Jin, T., Kou, J., et al. Lucas-Washburn equation-based modeling of capillary-driven flow in porous systems. Langmuir, 2021, 37(5): 1623-1636.

Cai, J., Perfect, E., Cheng, C., et al. Generalized modeling of spontaneous imbibition based on Hagen-Poiseuille flow in tortuous capillaries with variably shaped apertures. Langmuir, 2014, 30(18): 5142-5151.

Chen, Y., Xie, Q., Pu, W., et al. Drivers of pH increase and implications for low salinity effect in sandstone. Fuel, 2018a, 218: 112-117.

Chen, Y., Xie, Q., Sari, A., et al. Oil/water/rock wettability: Influencing factors and implications for low salinity water flooding in carbonate reservoirs. Fuel, 2018b, 215: 171-177.

Curtis, M. E., Ambrose, R. J., Sondergeld, C. H. Structural characterization of gas shales on the micro-and nano-scales. Paper SPE 137693 Presented at the Canadian Unconventional Resources and International Petroleum Conference, Calgary, Alberta, Canada, 19-21 October, 2010.

Dehghanpour, H., Lan, Q., Saeed, Y., et al. Spontaneous imbibition of brine and oil in gas shales: Effect of water adsorption and resulting microfractures. Energy & Fuels, 2013, 27(6): 3039-3049.

Fallahzadeh, S. H., Hossain, M. M., James Cornwell, A., et al. Near wellbore hydraulic fracture propagation from perforations in tight rocks: The roles of fracturing fluid viscosity and injection rate. Energies, 2017, 10(3): 359.

Fatahi, H., Hossain, M. M., Fallahzadeh, S. H., et al. Numerical simulation for the determination of hydraulic fracture initiation and breakdown pressure using distinct element method. Journal of Natural Gas Science and Engineering, 2016, 33: 1219-1232.

Fatahi, H., Hossain, M. M., Sarmadivaleh, M. Numerical and experimental investigation of the interaction of natural and propagated hydraulic fracture. Journal of Natural Gas Science and Engineering, 2017, 37: 409-424.

Feng, R., Chen, R., Sarmadivaleh, M. A practical fracability evaluation for tight sandstone reservoir with natural interface. The APPEA Journal, 2019, 59(1): 221-227.

Feng, Q., Xu, S., Xing, X., et al. Advances and challenges in shale oil development: A critical review. Advances in Geo-Energy Research, 2020, 4(4): 406-418.

Feng, R., Zhou, G., Sarmadivaleh, M., et al. The role of ductility in hydraulic fracturing: An experimental study. Paper ARMA 2018-442 Presented at the 52nd U.S. Rock Mechanics/Geomechanics Symposium, Seattle, Washington, 17-20 June, 2018.

Fjær, E., Holt, R. M., Horsrud, P., et al. Petroleum Related Rock Mechanics, 2nd Edition. Amsterdam, Netherlands, Elsevier, 2008.

Gale, J. F., Laubach, S. E., Olson, J. E., et al. Natural fractures in shale: A review and new observations. AAPG Bulletin, 2014, 98(11): 2165-2216.

Gale, J. F., Reed, R. M., Holder, J. Natural fractures in the Barnett Shale and their importance for hydraulic fracture treatments. AAPG Bulletin, 2007, 91(4): 603-622.

Gandossi, L., Von Estorff, U. An overview of hydraulic fracturing and other formation stimulation technologies for shale gas production. JRC86065, 2013.

Hossain, M. M., Rahman, M. Numerical simulation of complex fracture growth during tight reservoir stimulation by hydraulic fracturing. Journal of Petroleum Science and Engineering, 2008, 60(2): 86-104.

Hossain, M., Rahman, M., Rahman, S. Hydraulic fracture initiation and propagation: Roles of wellbore trajectory, perforation and stress regimes. Journal of Petroleum Science and Engineering, 2000, 27(3-4): 129-149.

Hou, B., Zhang, R., Zeng, Y., et al. Analysis of hydraulic fracture initiation and propagation in deep shale formation with high horizontal stress difference. Journal of Petroleum Science and Engineering, 2018, 170: 231-243.

Hubbert, M. K., Willis, D. G. Mechanics of hydraulic fracturing. Transactions of the American Institute of Mining and Metallurgical Engineers, 1972, 210: 153-166.

Josh, M., Esteban, L., Delle Piane, C., et al. Laboratory characterisation of shale properties. Journal of Petroleum Science and Engineering, 2012, 88: 107-124.

Kumagai, H., Chouet, B. A. Acoustic properties of a crack containing magmatic or hydrothermal fluids. Journal of Geophysical Research: Solid Earth, 2000, 105(B11): 25493-25512.

Li, Y., Liu, C., Li, H., et al. A review on measurement of the dynamic effect in capillary pressure. Journal of Petroleum Science and Engineering, 2022, 208: 109672.

Liang, C., Chen, M., Jin, Y., et al. Wellbore stability model for shale gas reservoir considering the coupling of multi-weakness planes and porous flow. Journal of Natural Gas Science and Engineering, 2014, 21: 364-378.

Liu, C., Zhang, L., Li, Y., et al. Effects of microfractures on permeability in carbonate rocks based on digital core technology. Advances in Geo-Energy Research, 2022, 6(1): 86-90.

Lu, G., Gordeliy, E., Prioul, R., et al. Modeling simultaneous initiation and propagation of multiple hydraulic fractures under subcritical conditions. Computers and Geotechnics, 2018, 104: 196-206.

Lu, Y., Zeng, L., Xie, Q., et al. Analytical modelling of wettability alteration-induced micro-fractures during hydraulic fracturing in tight oil reservoirs. Fuel, 2019, 249: 434-440.

Mayerhofer, M. J., Lolon, E. P., Warpinski, N. R., et al. What is stimulated reservoir volume? SPE Production & Operations, 2010, 25(1): 89-98.

Peng, T., Yan, J., Bing, H., et al. Laboratory investigation of shale rock to identify fracture propagation in vertical direction to bedding. Journal of Geophysics and Engineering, 2018, 15(3): 696-706.

Perkins, T., Kern, L. Widths of hydraulic fractures. Journal of Petroleum Technology, 1961, 13(9): 937-949.

Priest, S. D., Selvakumar, S. The failure characteristics of selected British rocks. London, Imperial College, 1982.

Rahman, M. K., Hossain, M. M., Rahman, S. S. An analytical method for mixed-mode propagation of pressurized fractures in remotely compressed rocks. International Journal of Fracture, 2000, 103(3): 243-258.

Rahman, M. K., Hossain, M. M., Rahman, S. S. A shear-dilation-based model for evaluation of hydraulically stimulated naturally fractured reservoirs. International Journal for Numerical and Analytical Methods in Geomechanics, 2002, 26(5): 469-497.

Rice, J. R. Mathematical analysis in the mechanics of fracture, in Fracture: An Advanced treatise, edited by H. Liebowitz, Academic Press, New York, pp. 191-311, 1968.

Roshan, H., Al-Yaseri, A. Z., Sarmadivaleh, M., et al. On wettability of shale rocks. Journal of Colloid and Interface Science, 2016, 475: 104-111.

Shen, Y., Ge, H., Li, C., et al. Water imbibition of shale and its potential influence on shale gas recovery-a comparative study of marine and continental shale formations. Journal of Natural Gas Science and Engineering, 2016, 35: 1121-1128.

Silva, M. R., Schroeder, C., Verbrugge, J. -C. Unsaturated rock mechanics applied to a low-porosity shale. Engineering Geology, 2008, 97: 42-52.

Verdugo, M., Doster, F. Impact of capillary pressure and flowback design on the clean up and productivity of hydraulically fractured tight gas wells. Journal of Petroleum Science and Engineering, 2022, 208: 109465.

Wang, Q., Chen, X., Jha, A. N., et al. Natural gas from shale formation-the evolution, evidences and challenges of shale gas revolution in United States. Renewable and Sustainable Energy Reviews, 2014, 30: 1-28.

Wang, D., Chen, M., Jin, Y., et al. Theoretical and experimental study on fracture network initiation and propagation in shale that considers the capillary effect. Journal of Natural Gas Science and Engineering, 2016, 34: 486-498.

Wang, J., Rahman, S. S. An investigation of fluid leak-off due to osmotic and capillary effects and its impact on micro-fracture generation during hydraulic fracturing stimulation of gas shale. Paper SPE 174392 Presented at the EUROPEC 2015, Madrid, Spain, 1-4 June, 2015.

Wattenbarger, R. A., Alkouh, A. B. New advances in shale reservoir analysis using flowback data. Paper SPE 165721 Presented at the SPE Eastern Regional Meeting, Pittsburgh, Pennsylvania, USA, 20-22 August, 2013.

Xu, M., Dehghanpour, H. Advances in understanding wettability of gas shales. Energy & Fuels, 2014, 28(7): 4362-4375.

Yilmaz, I. Influence of water content on the strength and deformability of gypsum. International Journal of Rock Mechanics and Mining Sciences, 2010, 47(2): 342-347.

Zhou, Z., Abass, H., Li, X., et al. Experimental investigation of the effect of imbibition on shale permeability during hydraulic fracturing. Journal of Natural Gas Science and Engineering, 2016, 29: 413-430.